RESEARCH ARTICLE

Proteomic analyses of serous and endometrioid epithelial ovarian cancers – Cases studies – Molecular insights of a possible histological etiology of serous ovarian cancer

Rémi Longuespée[1,2], Hugo Gagnon[1,2*], Charlotte Boyon[1,3], Kurstin Strupat[4], Claire Dauly[5], Olivier Kerdraon[6], Adesuwa Ighodaro[1,7], Annie Desmons[1], Jocelyn Dupuis[5], Maxence Wisztorski[1], Denis Vinatier[1,3], Isabelle Fournier[1], Robert Day[2] and Michel Salzet[1]*

[1] Université Nord de France, LSMBFA, MALDI Imaging Team, EA 4550, Université de Lille 1, SIRIC ONCOLILLE, Cité Scientifique, Villeneuve D'Ascq, France
[2] Institut de pharmacologie de Sherbrooke et Département de chirurgie/urologie, Faculté de médecine et des sciences de la santé, Université de Sherbrooke, Sherbrooke, Québec, Canada
[3] Hôpital Jeanne de Flandre, service de Chirurgie Gynécologique, CHRU de Lille, France
[4] Thermo Fisher Scientific (Bremen) GmbH, Bremen, Germany
[5] Thermo Fisher Scientific (France), Silic, Courtaboeuf, France
[6] Laboratoire d'Anatomie et de Cytologie Pathologiques, CHRU de Lille, Lille, France
[7] OWNIP fellow, SUNY College at Old Westbury, Old Westbury, NY, USA

Purpose: Epithelial ovarian carcinogenesis may occur de novo on the surface of ovarian mesothelial epithelial cells or from cells originating in other organs. Foreign Müllerian cell intrusion into the ovarian environment has been hypothesized to explain the latter scenario. In this study, MALDI MS profiling technology was used to provide molecular insights regarding these potentially different mechanisms.

Experimental design: Using MALDI MS profiling, the molecular disease signatures were established in their anatomical context. MALDI MS profiling was used on serous and endometrioid cancer biopsies to investigate cases of epithelial ovarian cancer. We then applied bioinformatic methods and identification strategies on the LC-MS/MS analyses of extracts from digested formalin-fixed, paraffin-embedded tissues. Extracts from selected regions (i.e. serous ovarian adenocarcinoma, fallopian tube serous adenocarcinoma, endometrioid ovarian cancer, benign endometrium, and benign ovarian tissues) were performed, and peptide digests were subjected to LC-MS/MS analysis.

Results: Comparison of the proteins identified from benign endometrium or three ovarian cancer types (i.e. serous ovarian adenocarcinoma, endometrioid ovarian adenocarcinoma, and serous fallopian tube adenocarcinoma) provided new evidence of a possible correlation between the fallopian tubes and serous ovarian adenocarcinoma. Here, we propose a workflow consisting of the comparison of multiple tissues in their anatomical context in an individual patient.

Received: August 3, 2012
Revised: October 9, 2012
Accepted: December 4, 2012

Correspondence: Michel Salzet, Université Nord de France, LSMBFA, MALDI Imaging Team, EA 4550, Université de Lille 1, Cité Scientifique, 59650 Villeneuve D'Ascq, France
E-mail: michel.salzet@univ-lille1.fr
Fax: +3320434054

Abbreviations: AR, antigen retrieval; **EOC**, epithelial ovarian cancers; **FFPE**, formalin-fixed, paraffin-embedded; **HC**, hierarchical clustering; **HES**, hematoxylin, eosin, and safranin; **STIC**, serous tubal intraepithelial carcinoma

*These are co-authors and have contributed equally to this study.

Colour Online: See the article online to view Figs. 1–7 in colour.

Conclusion and clinical relevance: The present study provides new insights into the molecular similarities between these two tissues and an assessment of highly specific markers for an individualized patient diagnosis and care.

Keywords:
Cases study / MS profiling / MALDI-MS imaging / Ovarian cancer / Proteomic network

Additional supporting information may be found in the online version of this article at the publisher's web-site

1 Introduction

The origin of epithelial ovarian cancers (EOC) is a critical clinical issue. Currently, patients with a mutation in the BRCA gene, who are at higher risk for EOC, are surgically treated with a prophylactic bilateral salpingo-oophorectomy, which is the complete removal of the ovary and fallopian tubes. This procedure decreases the patients' quality of life because the total removal of the ovaries induces menopause, consequently making those women infertile.

There are two hypotheses for the origin of EOCs, i.e. the intrinsic and extrinsic [1, 2]. Ovarian cancer may develop de novo from the mesothelial epithelial cells located on the surface of the ovary or from cells originating in other organs [1–3] (Fig. 1). If the Müllerian origin of serous ovarian cancer theory is valid, then the surgical removal of the junction of the fallopian tube and the ovary would reduce the risk of developing serous ovarian cancers to the same extent as a bilateral salpingo-oophorectomy. A fimbriectomy, which consists of the removal of the fallopian tube and the junction between the fimbria and the ovary, has been proposed by some surgeons [4] for patients who have BRCA mutations. The theory of de novo EOC appearance is supported by HOX gene expression, which regulates the Müllerian duct differentiation in epithelial ovarian cancer, but not in normal ovarian surface epithelium. The ectopic expression of the HOX genes in mouse ovarian surface epithelium leads to the development of tumors that resemble EOC. In this scenario, different HOX genes give rise to distinct EOC histological subtypes (i.e. Hoxa9 for serous, Hoxa10 for endometrioid and Hoxa11 for mucinous cancer [1]). However, several studies have reinforced the second and newer theory, and the principal types of ovarian cancer tissues share similar characteristics with normal Müllerian-type tissues. Serous cancer tissue strongly resembles fallopian tube tissue, endometrioid tissue is similar to endometrial tissue, and mucinous tissue resembles intestinal tissue [1–3]. Recent studies on serous adenocarcinoma, the most common type of ovarian cancer, have shown that 80% of these adenocarcinomas are associated with in situ cancerous lesions of the tubal epithelium called "serous tubal intraepithelial carcinoma" (STIC), which may be the source of ovarian cancer [5–12]. Moreover, genomic signatures that may be associated with STICs, such as mutations in the p53 gene, have been observed [13–19]. Additional studies have identified other common serous ovarian and fallopian tube cancer signatures, indicating that some Müllerian markers, such as PAX8, are commonly found in fallopian tubes and ovarian cancers and not in the mesothelial epithelium of the ovary. Further studies have shown that mesothelial markers such as calretinin are absent [17].

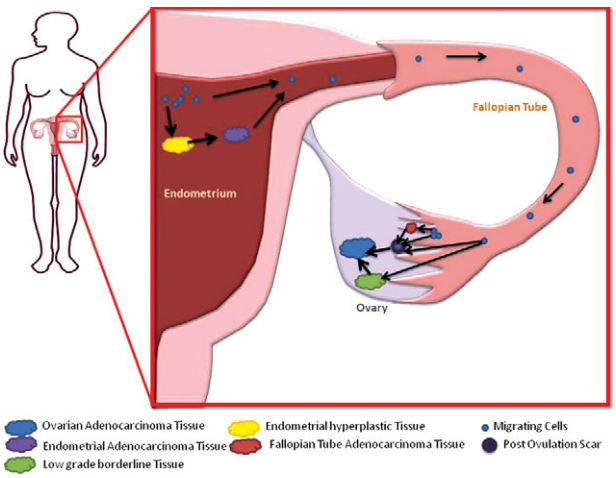

Figure 1. Recapitulation of the Müllerian origin of ovarian cancer type theories.Neoplastic processes may originate in Müllerian-related tissues and spread to the ovaries via postovulation scars or can directly evolve from benign cells. For endometrioid tissues, retrograde menstruation may play a role in disseminating cells from the endometrium to the ovaries. In serous cases, cells may come from the STICs evolving at the junctions between the fallopian tubes and the ovaries. Each tissue subtype and evolution grade is represented by a color that corresponds with the colors used for the PCA spectra spots in the following figures.

The origin of serous ovarian cancer is still under debate, but evidence elucidating the molecular nature of the tissues may be provided by mass spectrometric strategies. In the early 1990s, MALDI MS profiling, which consists of the direct molecular analysis of hundreds of biological compounds in tissues, was proposed [20]. Since the beginning of the last decade, many institutions have invested in molecular histological screening [20–25], including that of ovarian cancer samples [22, 25–31]. Thus, MALDI MS molecular profiling is considered a new and important "molecular histology" tool. We proposed to investigate the molecular nature of serous and endometrioid cancers using the novel MALDI MS profiling technology (Fig. 2A and B). This technology provides a comparison of the molecular profiles from different ovarian cancer tissues with the corresponding reference tissues.

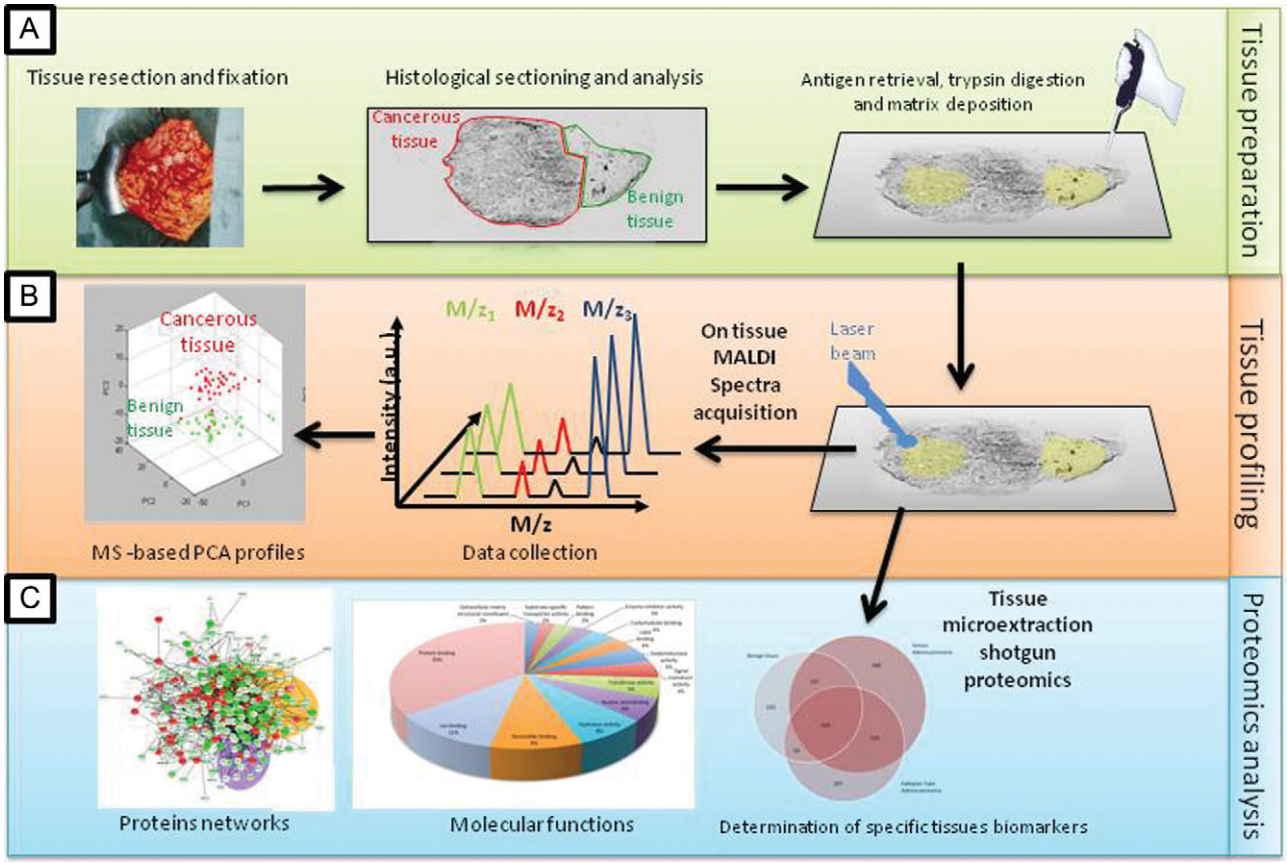

Figure 2. (A) The tissue preparation and analysis workflow for MALDI profiling and on-tissue proteomics. The resected organs or tissues were formalin fixed, paraffin embedded, and sliced with a microtome. The sections were mounted on conductive slides and dewaxed before antigen retrieval, the matrix was dropped onto the section, and the mass spectrometric analysis was performed on the tissue area. (B) The corresponding PCA of the tissue with normal and carcinomatous endometrium. The PC1/PC2, PC1/PC3, and PC2/PC3 analyses are shown, illustrating the best 2D-space separation of the ions. (C) After PCA analysis, the tryptic digests were extracted for the tissue sections by solvents washes. These digests were submitted to proteomic analyses. The use of specific software allowed us to determine the proteins' molecular functions and biological processes. It was also possible to elaborate the interaction networks of the proteins of interest.

In this present study, we first evaluated the use of MALDI MS on tissues on endometrioid low-grade ovarian cancer cases. Using PCA calculations on acquired spectra, we compared the global molecular profiles of the different tissues involved in the evolution of this pathology, i.e. between the endometrium and the ovaries.

This first examination allowed us to observe in a handly view of the global similitudes and dissimilitudes of endometrial and ovarian tissues.

The second part of the study is a more extensive analysis aiming to bring new clues for the tubal origin of serous ovarian cancer. Indeed, we first evaluated the global profiles of tubal and ovarian tissues by PCA analyses on MALDI MS spectra using the same procedure in the first part.

We then aimed to identify the potential molecular actors implicated in the close relationship between ovarian serous cancer tissues and tubal tissues. To do so, we performed a solvent-based extraction on previously analyzed regions of interest in the different tissues and conducted LC-Orbitrap MS analyses. The use of bioinformatics for analyzing the proteomics information allowed us to depict the common molecular functions for the cancerization of different organs and gave us access to the organs' specific molecular content (Fig. 2C).

2 Materials and methods

2.1 Materials

CHCA and TFA were obtained from Sigma-Aldrich and used without further purification. Trypsin was purchased from Promega. ACN p.a. and methanol p.a. were obtained from J.T. Baker.

2.2 Samples

Formalin-fixed, paraffin-embedded (FFPE) tissues were obtained from the CHRU de Lille pathology department. An institutional review approval (CPP Nord Ouest IV 12/10) was obtained without requiring informed consent from patients. The ethical committee considered contacting the patients, often many years after surgery, to be unnecessary. Our reference pathologist (O. K.) selected the FFPE blocks that included ovarian cancer tissue and tissue from the potential Müllerian precursor. To avoid interpatient variability, each figure in the Results section represents tissue from the same patient. The International Federation of Gynecology and Obstetrics stages for each specimen were determined, and the results of the histological examinations were recorded. For the histological imaging prior to MALDI analysis, 4-μm-thick tissue sections were cut from the FFPE whole-mount ovarian tissue blocks. The sections were placed on indium tin oxide-coated slides and heated for 60 min at 58°C [29]. The tissue was counterstained with hematoxylin, eosin, and safranin (HES), dehydrated using a graded ethanol series, and air-dried for histological examination by our staff pathologist. The tissues appeared heterogeneous and contained cancerous, hyperplastic, and normal regions, with stromal tissue in each region [29, 32].

2.3 HES staining

The following procedure was used for the HES staining. The sections were heated for 5 min, stained with hematoxylin for 3 min, rinsed with water, washed twice in a solution of 156 mL EtOH (95%), 44 mL H_2O, and 80 μL HCl, washed in water, washed in a solution of 0.48 mL NH_4OH (35%) and 200 mL H_2O, washed with water for 5 min, washed in ethanol (80%), colored with eosin for 10 s, washed twice with ethanol (95%), washed twice with ethanol (100%), stained with safranin (10 g/L in ethanol (100%)) for 6 min, and then washed twice in ethanol (100%) and once in xylene for 1 min [29, 33].

2.3.1 Tissue dewaxing

Ovarian FFPE tissues were used for the retrospective studies. Tissue sections (6 μm) were generated using a microtome and were placed on conductive glass slides coated with indium tin oxide on one side. The paraffin was removed by submersion in toluene twice for 5 min followed by a light rehydration in ethanol baths (100, 96, 70, and 30%) before the slides were dried in a desiccator at room temperature [29, 33].

2.3.2 Antigen retrieval

FFPE tissues have well-conserved tissue morphology and the capacity to prevent molecular degradation. Due to methylene bridge formation during conservation, trypsin digestion is often necessary to retrieve protein information. Because cross-linking continues over time in FFPE tissue blocks, protein accessibility becomes increasingly difficult. Enzymatic cleavage may be affected, which may lead to poor enzymatic yields. Therefore, it is necessary to establish processes that facilitate protein access, and many such protocols exist [33, 34]. However, the associated molecular changes of these so-called antigen retrieval (AR) processes remain poorly understood. The most reasonable hypothesis is that AR allows changes in the conformation of cross-linked proteins and thus facilitates access to sites within proteins. Due to the variation among protocols, systematic tests of different AR techniques are required for an optimized protocol, so several protocols were tested here. Citric acid AR provides good results with prostate tissue sections [33]. Citric acid AR protein unmasking was performed by immersing the slides in 10 mM of citric acid for 20 min at 98°C and drying them in a desiccator for 10 min. Prior to enzymatic digestion, the slides were incubated twice in 10 mM NH_4HCO_3 to remove the remaining AR solution and condition the tissue for effective enzyme activity.

2.4 Trypsin digestion and matrix digestion

Ten milliliters in total of a solution containing 40 μg/mL trypsin in 50 mM ammonium bicarbonate was dropped onto each tissue discrete region of interest using gel loader tips (the 10 μL have been dropped in 5 times using 2 μL of solution). This procedure avoids the drop to spread and thus to have a mixed up of different cell types. The slides were then incubated for 4 h at 37°C in a customized humidity chamber (a 10 cm × 15 cm box filled with water to one quarter of the box height and placed in a 37° incubator). After the trypsin digestion, 10 μL of a 10 mg/mL CHCA solution in aqueous TFA 0.1%/ACN (3:7) was dropped onto each section [35, 36].

2.5 MALDI MS profiling methodology

The MS profiling approach is presented in Fig. 2A and B [22, 25]. The first step includes the sectioning and preparation of tissue using standard methods. The preservation of tissue integrity while avoiding molecular composition changes (e.g. enzymatic activation) is of utmost importance. The second and third steps are based on MALDI-MS technology. The second crucial step is the deposition of the matrix onto the tissue section. The importance of the matrix for mass spectra quality is well established, and the proper matrix choice is crucial for a successful MALDI experiment. It is also important that the MALDI-MSI matrix does not induce molecular delocalization across the tissue sample. Such delocalization must not spread further than the area analyzed by one laser pulse. The third step is the tissue data acquisition. This step depends on the mass analyzer and involves optimizing various parameters; the acquisition step requires the automation

of the analytical process. The final step consists of data processing via informatics tools.

2.6 Tissue profiling using MALDI

For each tissue, 50 spectra were acquired on spots homogeneously distributed across the analysis surface. The profiles were acquired using an UltraFlex II MALDI-TOF/TOF instrument (Bruker Daltonics, Bremen, Germany) equipped with a smart beam laser with a 200 Hz repetition rate and controlled by FlexControl 2.5 software (Bruker Daltonics). The mass spectra profiles were acquired in the positive reflection mode in the 500–5500 Da mass range. One thousand spectra were acquired at each position using a 200 Hz laser frequency. The images were recorded and reconstructed using FlexImaging II 2.5 software (Bruker Daltonics).

2.7 Statistical data analysis

The data obtained using FlexImaging II 2.5 software (Bruker Daltonics) were loaded into the ClinProTools v2.5 software (Bruker Daltonics) to conduct PCA and hierarchical clustering analysis. After standardization of the data, the unsupervised PCA method was selected. The PC1 and PC2 components were found to have the largest variance [33, 37].

2.8 LC-MS/MS Analyses

Trypsin-digested peptides from the FFPE tissue after the antigen retrieval procedure were manually extracted from specific tissue regions after PCA. Using a micropipette, specific regions were subjected to 20 successive washes with 100 μL of 80% ACN in water. The extract solution was then dried with a SpeedVac (Savent). The dried peptides were redissolved in 10 μL 0.1% TFA. The salts were removed from the solution, and peptides were concentrated using a solid–phase extraction procedure with a Millipore ZipTip device in 10 μL 80% ACN elution solution. The solution was dried again using a SpeedVac, and the dried samples were resuspended in a solution of 5% ACN and 0.1% formic acid. The samples were separated by online reversed-phase chromatography using a Thermo Scientific Proxeon Easy-nLC system equipped with a Proxeon trap column (100 μm id × 2 cm, Thermo Scientific) and a C18 packed-tip column (100 μm id × 15 cm, Nikkyo Technos Co.) [38]. The peptides were separated using an increasing concentration of ACN (5–40% over 110 min) at a 300-nL/min flow rate. The LC eluent was electrosprayed directly from the analytical column, and a 1.7 kV voltage was applied via the liquid junction of the nanospray source. The chromatography system was coupled to a Thermo Scientific Orbitrap Elite mass spectrometer, which was programed to acquire in a data-dependent mode. The survey scans were acquired in the Orbitrap mass analyzer operating at 120 000 (FWHM) resolving power. A mass range of 400–2000 m/z and a target of 1E6 ions were used for the survey scans. The precursors observed with an intensity of over 500 counts were selected "on the fly" for the ion trap CID fragmentation with an isolation window of 2 amu and a normalized collision energy of 35%. A target of 5000 ions and a maximum injection time of 200 ms were used for CID MS^2 spectra. The method was set to analyze the 20 most intense ions from the survey scan, and a dynamic exclusion was enabled for 20 s. Each sample has been analyzed three times. The limit of detection of the instrumentation is 25 000 peptides for an LC-MS/MS run.

2.9 Analysis

Tandem mass spectra were processed using the Thermo Scientific Proteome Discoverer software version 1.3. Resultant spectra were matched against the Swiss-Prot® Human database (version January 2012) using the SEQUEST® algorithm. The search was performed by selecting trypsin as the enzyme with two missed cleavages allowed. The precursor mass tolerance was 10 ppm, and the fragment mass tolerance was 0.5 Da. *N*-terminal acetylation, methionine oxidation, and arginine deamination were set as the variable modifications. Peptide validation was performed using the Percolator algorithm. The peptides were filtered based on a q-value of 0.01, which corresponds to a 1% false discovery rate.

Only proteins with a score of over 5, which represents the proteins identified with two or more unique peptides, were kept for analysis. The relative protein expression was calculated based on the protein score, which was shown to be an adequate relative indicator of the relative differential expression [39, 40]. We compared the acquired results with an analysis using the Scaffold 3 software [41]. We considered this method to be quite accurate because it gave similar results when a quantitative comparison of the different tissues' proteins relied on spectral counting (data not shown). Gene ontology analysis was performed using Blast2Go [42]. The network analysis was performed as follows: The gene names of identified proteins were used as input to retrieve a network from STRING [43], and this network was then loaded into Cytoscape 2.8 [44] with relative expression data using Id mapper. The Reactome FI pluggin was used to select a sub network of gene ontology terms and NCI database-associated disease-specific proteins.

3 Results and discussion

The study presented here is composed of two separated parts. The first one consists in the determination of molecular signatures of tissues from patients afflicted by low-grade endometrioid cancers, using PCA calculations applied to mass spectra. A solvent extraction has then been performed on the

ovarian endometrioid cancer tissue, followed by a LC MS/MS analysis. This analysis has been used to support the second part of the investigation.

The second part of the investigation consists in the examination of serous cancer cases. We also present the molecular profiles of the different tissues. We then focused on one case to perform an extensive proteomic analysis comparing different tissues of interest. This part of the study is devoted to the finding of clues of the potential tubal origin of ovarian cancer in this specific clinical case.

Before any analysis, we aimed for the proper selection of the tissues areas for the molecular comparisons. The methods presented here allowed us to make the examination of the molecular content of whole tissue areas without fastidious steps of laser capture microdissections for cell types selections. In order to avoid any analytical artifacts due to the analysis of mixed cells types, a first meticulous tissue area selection have been performed by our reference pathologist (O. K.). Between any tissues to compare, we aimed to have the same amount of vessels. For normal tissue tubal, ovarian, and endometrial tissues, we selected representative regions of interest of the whole tissue areas, i.e. with the average proportion of stromal and epithelial cells. For cancerous tissue area selection, we also aimed for the selection of ROI with average proportion of cancerous epithelia and surrounding stromal cells.

The cancerous epithelia proportion is the most represented cell types (80–90% of the cells types), and absolutely absent from the other tissues which are by almost 100% stomal cells. We then estimate that the comparison of the cancerous tissues with normal tissues controls is free of the analytical artefacts that we could have without a previous selection of the tissues.

3.1 Part 1: Molecular signature profiling and proteomic analysis of endometrioid ovarian cancer tissues

In this first part of the investigation, we selected low-grade endometrioid tissues in order to test the feasibility of the PCA procedure to compare molecular profiles of selected tissues of interest. Indeed, we compare the possible similitude and dissimilitude between normal, cancerous, hyperplastic endometrium with borderline and cancerous ovaries tissues that our pathologist found for this case.

Due to the large amount of data acquired using the MALDI MSI method, data reduction and multivariate analyses were necessary to extract the information of interest. Among the multivariate methods available, PCA provides a proven method for automatic feature extraction [26, 33, 37]. Several studies have shown that PCA is a data reduction method that is useful for MALDI MSI in disease applications [26, 33, 37, 45, 46]. Therefore, PCA was applied to the data from several spectral acquisitions. In this bioinformatics spectral data processing, each peak was considered to be a single dimension, and each group of spectra was considered to be a multidimensional space. This process reduces the multidimensional space to two or three dimensions. The PCA approach provides access to *m/z*, which demonstrates differences between or within samples (Fig. 2B). PCA is often combined with hierarchical clustering (HC) because HC classifies the mass spectra according to similarities between their profiles, thus highlighting the regions containing differing molecular content. In these ways, the different molecular content profiles may be easily compared among the different tissue types. As shown in Supporting Information Fig. 1, the mass spectra observed in normal, borderline, and adenocarcinoma ovarian tissues contain a high number of peaks that appear to present some intensity differences that could not be precisely quantified manually. PCA analysis thus evaluates the relative intensity of all peaks and provides insight into differential molecular signatures.

The correlations between each cellular phenotype were tracked across the *m/z* detected in each tissue type. The endometrioid cancer origin hypothesis posits that cells from retrograde menstruation and endometriosis or endometriotic cysts reach the ovary, develop in the endometrial tissue and eventually become cancerous [47]. For each case, the ovarian biopsy was studied concurrently with its respective case-matched control (i.e. the endometrial tissues). We focused on the cases whose endometrioid cancers were associated with endometrial lesions (Fig. 3). HES staining and pathological analysis were used to study the FFPE sections from different organs of the same patient. To facilitate the analysis and determine the nature of the tissues, we retained the annotations added by the pathologist on the tissue section slides.

Two patients were selected because they presented with ovarian endometrioid and endometrial cancers or hyperplasic lesions. These tissue sections included borderline (BL) ovarian tissue (in green) and a portion of an adenocarcinoma (ADK, in blue) (Fig. 3), endometrial tissue (in yellow) (Fig. 3) and its contralateral normal ovary tissue (in red) (Fig. 3), and adenocarcinomatous or hyperplastic endometrial tissues (in purple). Adjacent sections were subjected to the MALDI profiling procedure after citric acid antigen retrieval and trypsin digestion to unmask the peptide and protein markers. PCA was performed for each region of interest in the sections; the data are presented in Fig. 3 for the two patient cases in the A and B insets. Figure 3A depicts the analysis of the first patient. Borderline (green) and cancerous (blue) tissue sections were found in the carcinomatous ovary (Fig. 3A1). These tissues were compared with normal endometrium (Fig. 3A2), carcinomatous endometrium (Fig. 3A2), and normal contralateral ovary (Fig. 3A3). For this patient, the normal endometrium is weakly proliferative. In this case, it is easy to distinguish the spectral profile scatters in the regions of interest, which are circled in the same colors used to highlight the HES scan sections. The profiles have a specific order in 2D space, which is determined by the first PCs (i.e. PC1 and PC2), ranging from normal endometrial tissue to ovarian carcinoma. Endometrial carcinoma showed close similarities with normal endometrial

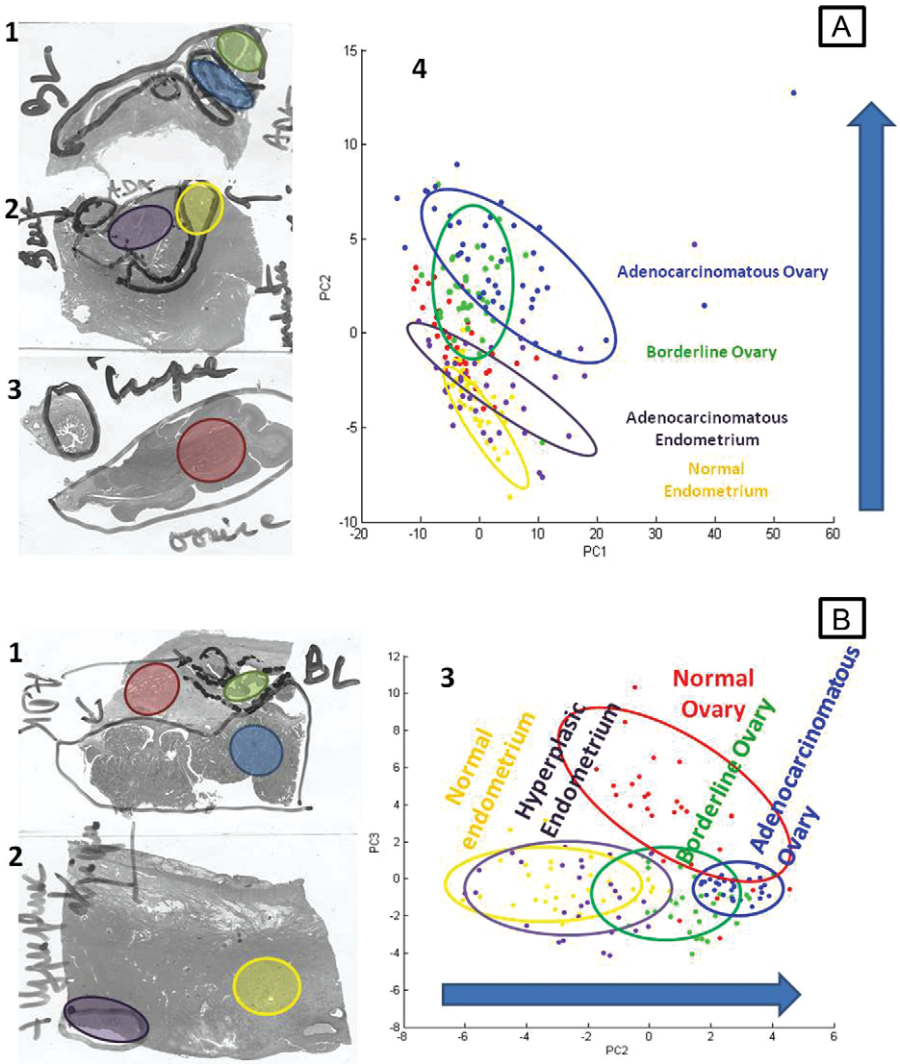

Figure 3. PCA analysis of the two patient tissues with endometrioid ovarian cancer. Citric acid AR was applied to FFPE tissue sections. Ten microliter trypsin droplets were then deposited on each tissue region of interest (ROI) and HCCA matrix. Fifty MALDI/TOF spectra were then acquired for each region of interest, and the acquired data were submitted to PCA for a molecular-based comparison. (A) First patient case, HES sections (1, 2, 3) and PCA analyses of normal, adenocarcinomatous ovarian tissues, and normal and adenocarcinomatous endometrial tissues (4). (B) Second patient case, HES sections (1, 2) and PCA analyses of normal, borderline, and adenocarcinomatous ovarian tissues and normal and hyperplasic endometrial tissues (3).

tissue (Fig. 3A4). It seems that normal and adenocarcinomatous endometrial tissues share common ions with borderline ovarian tissue and that borderline ovarian tissue share common ions with and adenocarcinomatous ovarian tissue. In this context, the blue arrow represents a possible continuum in the different molecular contents of the tissues through the different organs and tissue types.

The inset in Fig. 3B demonstrates the analysis of the second endometrioid ovarian cancer case.

In this second case, we found normal, borderline, and carcinomatous tissues in the ovarian biopsy sections (Fig. 3B1). Is this case, the patient present an atrophic normal endometrium. In parallel, this patient presented with an atypical hyperplastic zone detected near the endometrial tissue that was considered a region of interest (Fig. 3B2). We found that the PC2–PC3 dimensions indicated a close similitude in the molecular profiles of the normal endometrial and hyperplastic tissues (Fig. 3B3). In this case, the normal ovarian molecular profile was different from the preinvasive and invasive profiles. In the 2D PC space, the molecular-based profiles of the ovarian borderline and carcinomatous tissues were placed after the hyperplastic endometrial tissue. From these observations, we suggest that endometrial hyperplasia may be a latent state for carcinoma progression. With this global molecular information, we predict that an endometrial hyperplasic cell may nest in the ovarian environment and evolve to borderline and lead to a carcinomatous state.

A solvent extraction of the tryptic peptides from the endometrial adenocarcinoma has then been performed and LC-MS/MS analyses as mentioned in Section 2. These analyses have then been used in Part 2 (see Section 3.2).

These results gave us insights in the histological resemblance between the tissues involved in endometrioid ovarian cancer progression, and in the possible histological etiology of this type of cancer. We also got a first clue of the usefulness of this method for the evaluation of this specific issue.

3.2 Part 2: Molecular signature profiling of the tissues and proteomic analysis of serous ovarian cancer tissues: insights of a possible histological origin

In this part, we focused on serous ovarian cancers because the proof of a fallopian tube tissue origin may represent the most relevant context for further clinical application. Furthermore, serous ovarian cancers represent the most prevalent cases. We then applied the MALDI profiling method on serous ovarian cancer tissues. The results of these analyses are presented in Fig. 4. The tissue regions of interest are labeled pink for the normal fallopian tube, red for normal ovary, blue for ovarian adenocarcinoma, and turquoise for tubal adenocarcinoma (Fig. 4). Three patient cases were selected. For a more defined view of the molecular profiles, we added the hierarchical clustering results of the tissues of interest.

The first patient did not present with any tubal lesions. Therefore, we aimed to compare the ovarian carcinomatous regions with the normal fallopian tube tissue. The tubal origin of serous ovarian tissue theory also states that a normal cell from the fallopian tube may evolve into cancer in the ovarian environment.

The first case is presented in the inset in Fig. 4A. The PCAs in the first two axes (Fig. 4A2) demonstrated that the normal fallopian tube and normal ovarian tissues presented similar molecular profiles that were different from normal contralateral ovarian tissue. The HC data demonstrated that the fallopian tube spectra presented an intermediate profile that was between the ovarian cancer and normal ovarian tissue profiles (Fig. 4A3).

The last patient presented in the inset in Fig. 4B presented a fallopian tube adenocarcinoma (Fig. 4B1 and B2). The patient has been diagnosed for the presence of adenocarcinomatous cells after gynecological examination. A diagnostic coeliscopy revealed the presence of carcinomatous annexes. A radical annexectomy has been performed in both the tubal and the ovarian tissues have been analyzed by the pathologist. After the microscopic examination, the pathologist stated that the tube, that have been taken in totality, presented an invasive adenocarcinomatous proliferation, mostly solid, measuring 8 mm in length on the longer axe. Otherwise the fimbria was dotted with STIC (Fig. 5). The pathologist clearly stated that ovarian lesion corresponded to a metastasis of the tubal adenocarcinoma.

The PCA (Fig. 4B3) shows that ovarian cancer presents the following order of molecular profiles: normal ovary, normal fallopian tube, fallopian tube adenocarcinoma, and ovarian serous adenocarcinoma. This observation is in agreement with the molecular origin of ovarian cancer theory. HC (Fig. 4B4) also confirms the similar characteristics among ovarian adenocarcinoma and fallopian tube adenocarcinoma and normal tissues.

These analyses were easy to perform and allowed a quick survey on the global differential molecular content between the tissues. Therefore, because the identification of the proteins responsible for molecular differentiation is difficult to obtain using the MALDI TOF device, we performed an in-depth analysis of the molecular content of the tissues of interest in the serous ovarian cancer case.

3.2.1 Proteomics analyses of serous ovarian cancer and tubal cancer tissues

For the proteomics analyses, peptide extractions from normal endometrium and endometrioid ovarian cancer of the case presented in Fig. 4B were performed, and peptide digests were then subjected to LC-MS/MS analyses.

Among the identified proteins, those with a score under 5 were removed for subsequent analyses because they were identified from the MS/MS to have less than two peptides. We then evaluated the number of common proteins between the tissues of interest. Each accession number, proteins description, gene name, and relative score associated with the selected proteins are reported in Supporting Information Table 1. The selected tissues are serous ovarian adenocarcinoma, fallopian tube serous adenocarcinoma, and benign ovarian tissues. The Venn diagram presented in Supporting Information Fig. 2 illustrates the common identification between each cancer tissue. The obtained overlapping identifications provide an insight into the molecular similarities of the tissues. Primarily, the number of specific proteins in the serous ovarian adenocarcinoma samples appears higher than any of the other specific proteins, suggesting that many cellular processes involving several proteins may be mandatory for ovarian cancer progression. The number of proteins in the two other cancers was similar. We then observed that the number of common proteins identified between serous EOC and fallopian tube serous cancer was higher than that between the endometrioid EOC type, and the number of common proteins identified between endometrioid EOC and tubal cancer was more than threefold less than that between serous EOC and fallopian tube serous cancer. These observations suggest that serous EOC has a molecular profile that is more similar to tubal cancer than any other type of EOC. This point also supports the ectopic origin of EOC hypothesis. Although these data provide interesting information regarding the relative molecular nature of each cancer, this comparison lacks accuracy because it relied on two patient cases. Thus, the comparison may be partially influenced by the interpatient variability.

We then focused on a single patient case of ovarian serous cancer. We compared the tissues of interest illustrated in Fig. 4B.

The Venn diagram in Fig. 5A demonstrates the common identified proteins in benign ovary, serous ovarian cancer, and serous tubal cancer for the same patient. As illustrated, more proteins are shared in common between tubal cancer and serous ovarian cancer than between serous cancer and the benign ovary. This may suggest that processes implicated in serous related cancers (i.e. ovarian and tubal) require

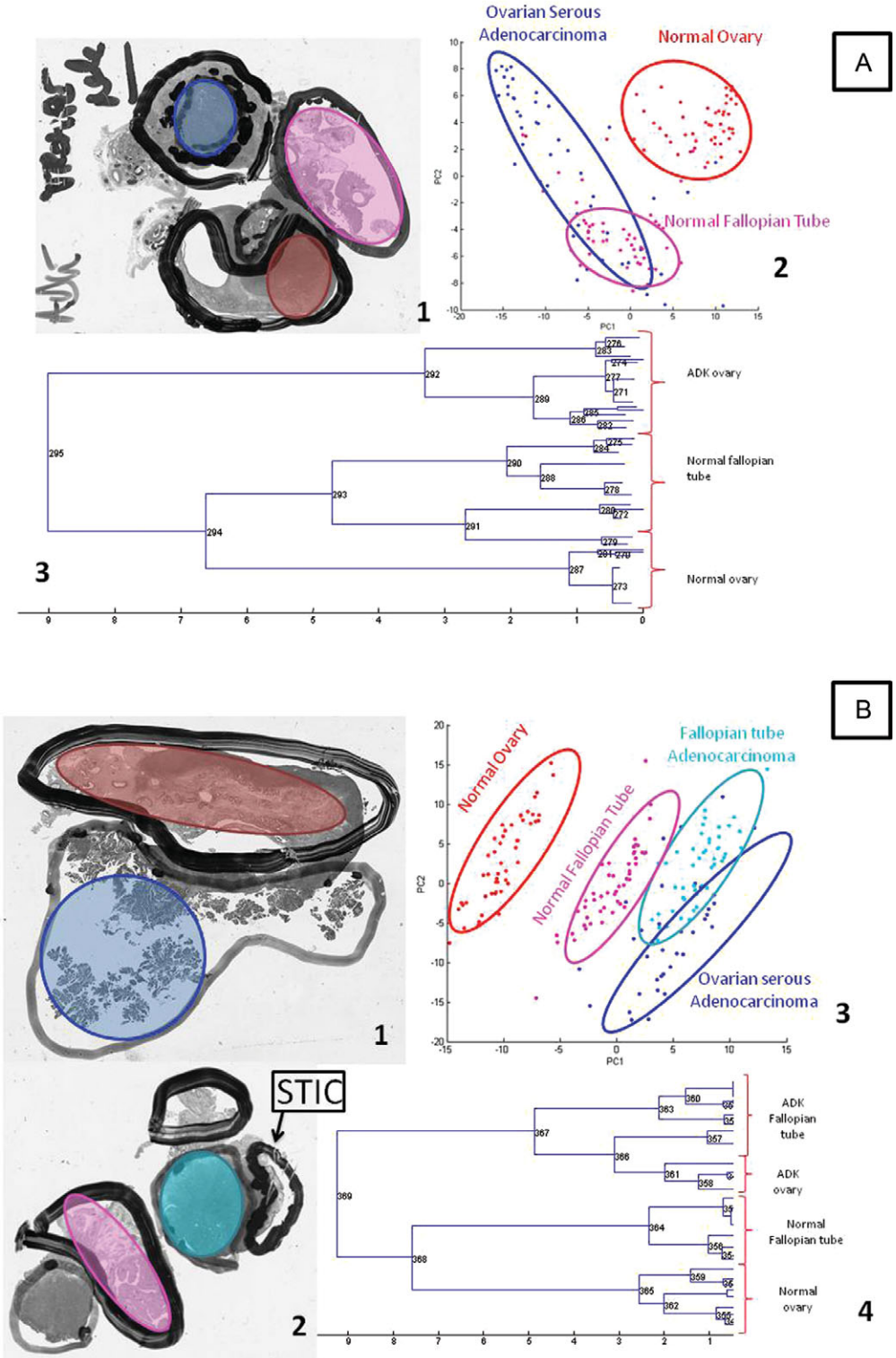

Figure 4. PCA analysis of the two patient tissues with serous ovarian cancer. Citric acid AR was applied on FFPE tissue sections. Ten microliter trypsin droplets were then deposited on each tissue region of interest (ROI) and HCCA matrix. Fifty MALDI/TOF spectra were then acquired for each region of interest, and the obtained data were submitted to PCA for a molecular-based comparison. (A) First patient case, HES sections (1), PCA analyses of normal, and adenocarcinomatous ovarian tissues and normal tubal tissue (2), HC of spectra (3). (B) Second patient case, HES sections (1, 2) and PCA analyses of normal and adenocarcinomatous ovarian tissues and normal and cancerous fallopian tissue (3,4).

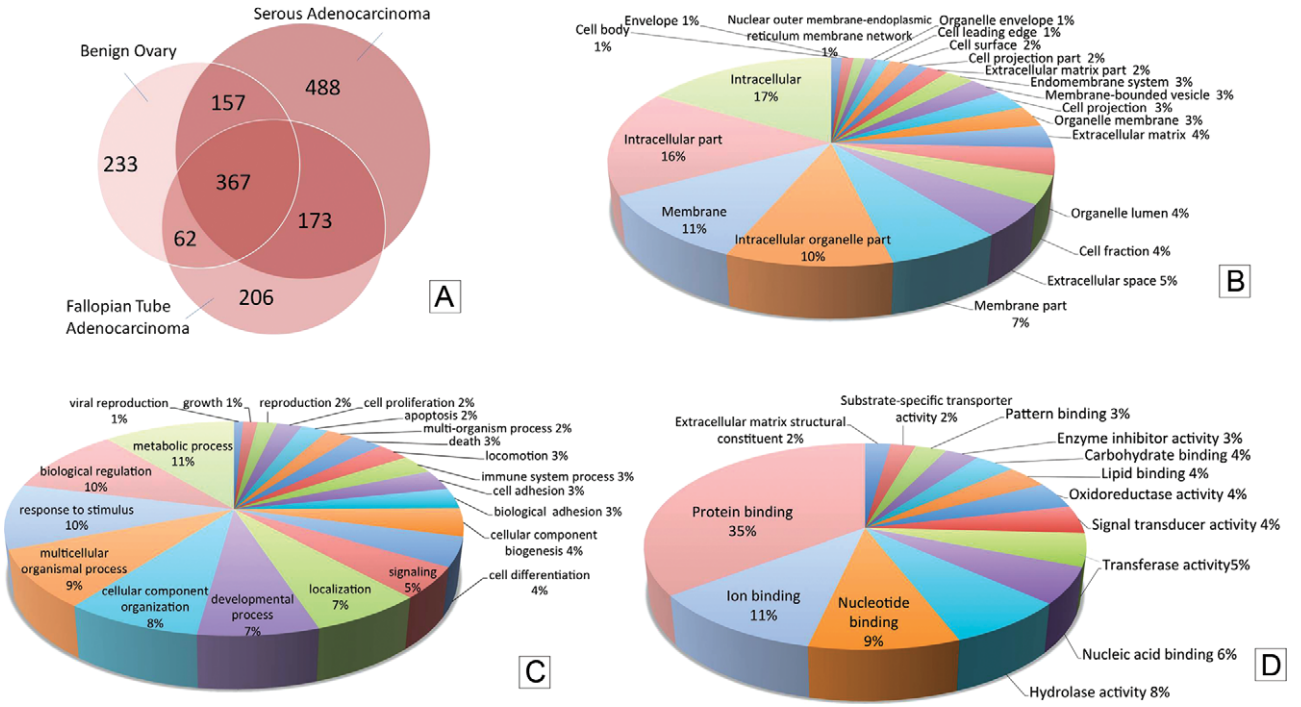

Figure 5. Analysis of common proteins identified by LC-MS/MS between serous ovarian and tubal cancers. Venn diagram of protein IDs from ovarian, tubal cancer, and normal ovarian tissues in the same patient case (A). Blast2Go was then used to determine the gene ontology of proteins with similar ID scores between the ovarian cancer and fallopian tube cancer tissues, and pie charts for cellular localization (B), cellular processes (C), and molecular functions (D) were drawn.

numerous molecular actors, and a portion of these is in common between ovarian and tubal serous cancers.

The protein identification (ID) score was compared between the different tissue regions. The differential protein IDs between ovarian cancer and benign tissues were selected as proteins specifically implicated in the cancerous processes. Some of these demonstrated highly similar ID scores between ovarian cancer and fallopian tube cancer tissues. These proteins were selected as proteins possibly implicated in ovarian and tubal serous cancers processes.

The molecular function of each of the specific proteins was determined using Blast2GO. Figure 5 shows pie charts demonstrating the proteins' cellular localization (Fig. 5B), the biological processes in which they are involved (Fig. 5C) and their molecular functions (Fig. 5D). In these representations, we observed that the functions principally found in common between ovarian and tubal cancer have been found in other cancers. Therefore, we demonstrated that the major molecular functions were related to molecular binding, with 35% of protein binding, and metabolism (Fig. 5D). With regards to cellular processes (Fig. 5C), the most represented corresponds with well-known processes associated with cancer. Processes such as growth, cell proliferation, cellular component organization, biological adhesion, response to stimulus and signaling and metabolic processes correspond with classically described functions in tumorigenesis phenomena. These elements provide an initial clue to the underlying mechanisms related to these two cancers.

All of these proteins have been reported in a network representing the functional interaction between these proteins based on the String database interaction probability (Fig. 6). In this network, a score based on the up- and downregulation of each of the proteins in common with ovarian and tubal cancers compared with the normal ovary is represented by a color code; the green shade represents negative score changes, and the red shade represents positive score changes. Thus, we postulated that this change in the score ranking reflects expression changes, i.e. a negative score change represents downregulation (green), and positive score change represents upregulation (red). From this global network (Fig. 6A, zoom in Supporting Information Fig. 3), subnetworks can be extracted, corresponding to proteins with functions of interest or related to physiopathological events. The first observation was that downregulation is predominant compared with upregulation. The framed subnetwork represents proteins associated with the NCI disease index (http://www.cancer.gov/), and they were selected using the Cytoscape-implemented Reactome FI plugin. Almost all of the selected proteins were found to be involved in neoplasms (Fig. 6B). A number of these proteins have also been found in female reproductive system neoplasms (Fig. 6C), particularly in ovarian cancer neoplasms (Fig. 6D). Among the upregulated proteins, we found chaperones, cell structure proteins, and proteins involved in DNA replication. The downregulated proteins correspond to other types of chaperone, adhesion, and structural proteins.

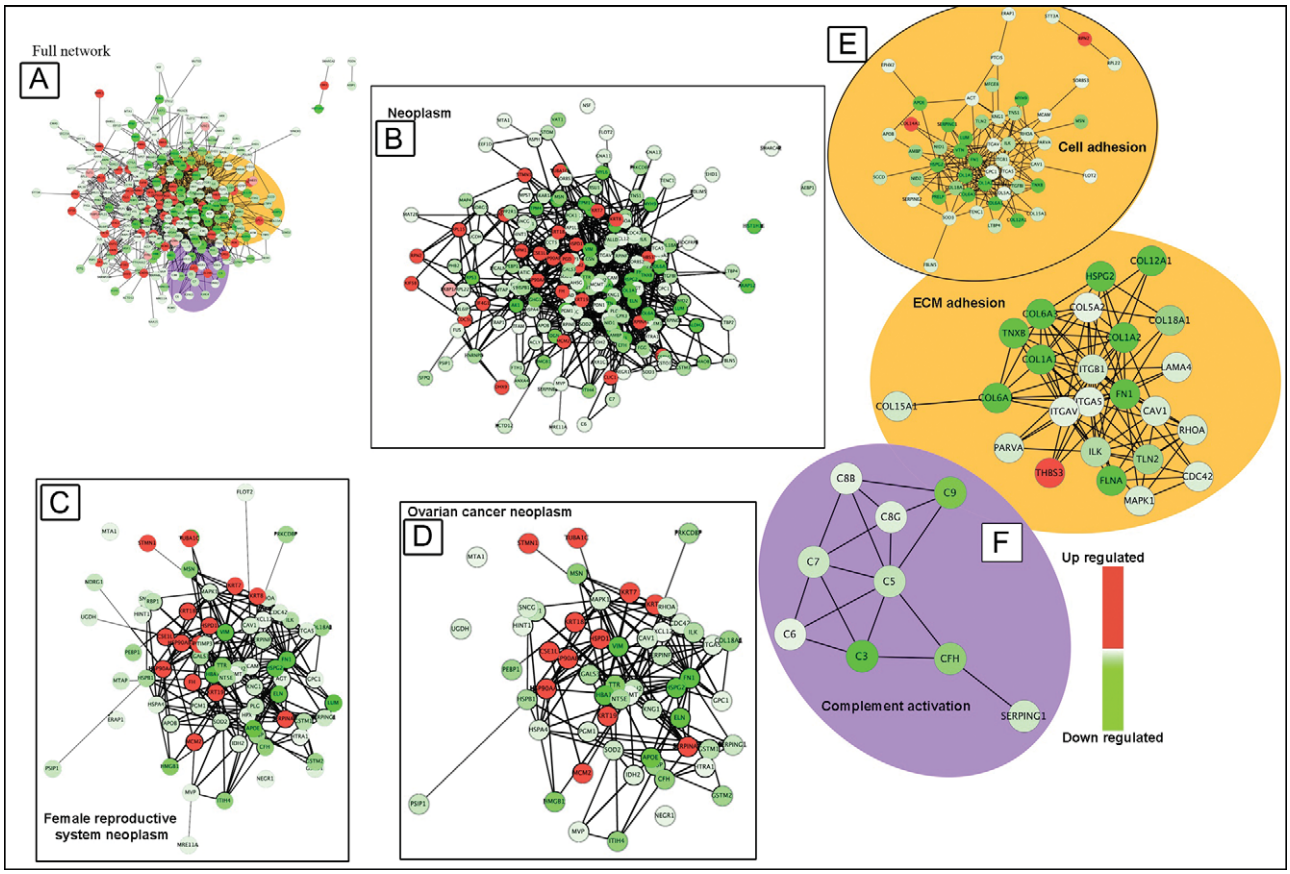

Figure 6. Interaction networks of proteins common between serous ovarian and tubal cancers. Interactions were retrieved using gene names in the STRING network database (A). A full network was then constructed using Cytoscape with relative expression data as the Id mapper; the score based on the up and downregulation of each of the common proteins between ovarian and tubal cancers compared with the normal ovary is represented by a color code with the green shade representing negative score changes and the red shade positive score changes. The Reactome NCI plugin was then used to draw subnetworks for neoplastic proteins (B), female reproductive neoplasm proteins (C) and ovarian cancer proteins (D). Blast2GO molecular functions were then used to represent networks for cell adhesion (E) and innate immune system proteins (F).

From these data, the molecular functions of interest were selected to construct subnetworks (Fig. 6, insets at right). We decided to draw the networks of the proteins for which the functions were mainly represented, namely cellular adhesion (yellow-orange inset, Fig. 6E). Many of these proteins appear downregulated. This corresponds to the metastatic behavior of the cancerous cells [48]. Indeed, in a spatio-temporal context, an EOC cell can detach from its tissue environment and attach to a new site. During these events, the plasma membrane of the cell loses its surface adhesion proteins for detachment. These observations highlight the common process mechanisms of ovarian and fallopian tube cancer tissues. According to the ectopic origin of ovarian cancer theory, a tubal cancerous cell could detach from its tumor site and attach in the ovarian environment. Another interesting molecular function observed in this network representation is complement activation (purple inset, Fig. 6F). We also found proteins associated with this function that was downregulated in the ovarian and tubal cancer contexts. This downregulation is also in agreement with previous discoveries. Previous work has shown that there is an immunosuppression phenomenon associated with ovarian cancer [48,49]. Here, complement activation proteins, namely the complement proteins C3, C5, C6, C7, C9, the complement component C8 gamma and beta chains (C8B, C8G), the complement factor H, and the plasma protease C1 inhibitor (SERPING1) (Supporting Information Table 3) were downregulated in the ovarian cancer context. Assuming that EOC has a Müllerian origin, it is not difficult to imagine that the suppression of the innate immune response is mandatory for a tubal cell settling in the ovary. A foreign cell could then act as an undetectable parasite in the ovarian immune environment. This mechanism would also be necessary for the evolution of these same cancerous cells in the fallopian tube environment.

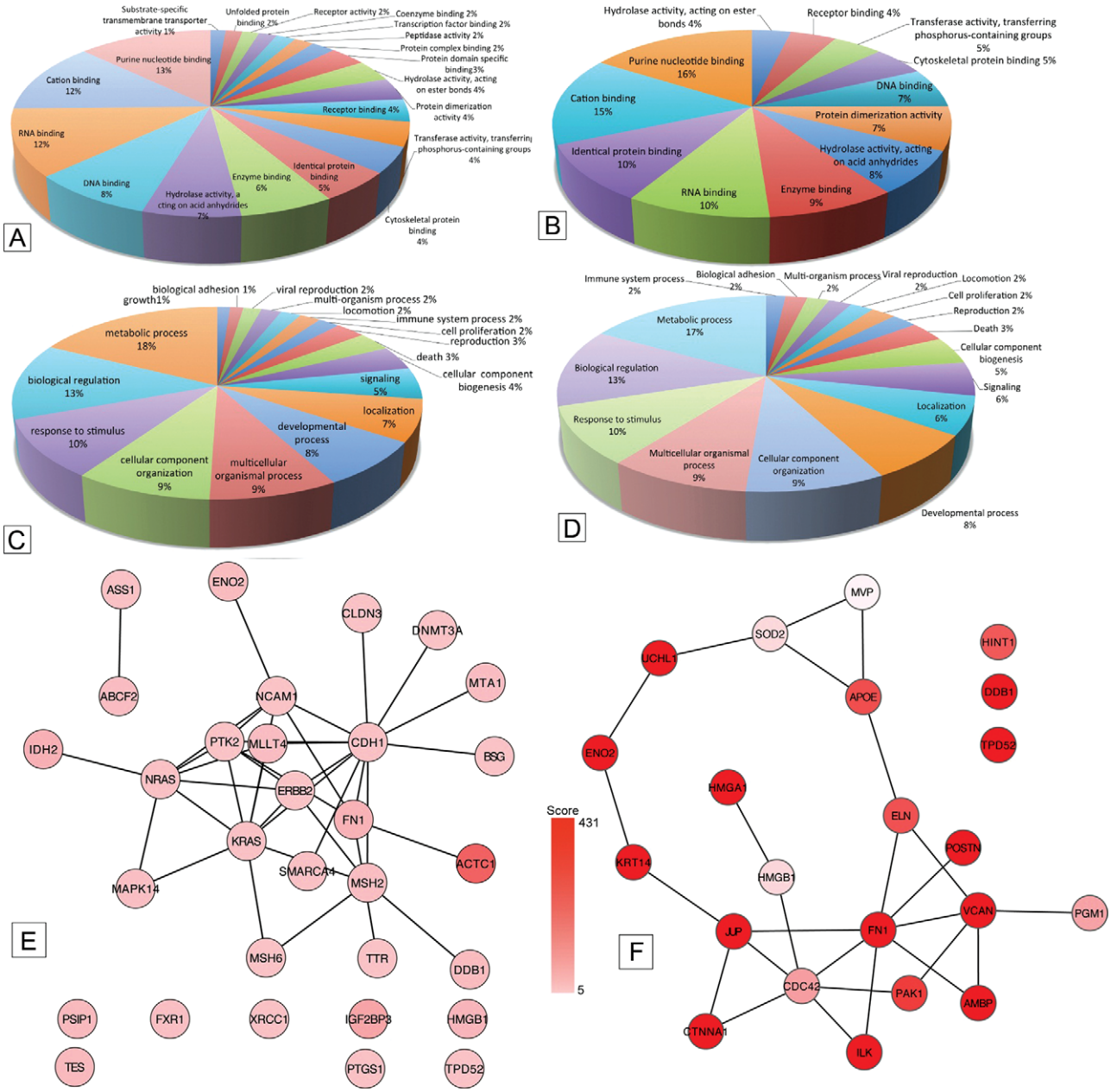

Figure 7. Analysis of specific proteins from fallopian tube and serous ovarian cancers. From Blast2GO annotations, pie charts representing the molecular functions of ovarian cancer proteins (A) and tubal cancer proteins (B), and the cellular processes of ovarian cancer proteins (C) and tubal cancer proteins (D) were drawn. Using the Reactome NCI plugin, known ovarian cancer marker networks were traced from the ovarian cancer (E) and tubal cancer networks (F).

To confirm the biological mechanistic found between ovarian a tubals cancer, we aimed to evaluate the proteins that were specifically found in both cancers but not in normal ovarian tissue. The distribution of the cellular processes was almost the same. Moreover, we found an overexpression of cytosqueletal proteins in ovarian cancer samples. We also found immunoproteasome activators such as PA28 alpha, which are known to be overexpressed and degraded in the ovarian cancer context [29, 49].

In addition to the inspection of the common molecular mechanisms of ovarian and tubal cancers, we examined the specific molecular mechanisms of ovarian and tubal cancers. Two arguments support this investigation. First, the analysis of tubal cancer proteins may provide insight into the underlying events in the fallopian tube environment that could lead to the metastasis of cancerous cells in the ovarian environment. In addition, investigation of specific serous ovarian cancer proteins may elucidate the mechanisms for cancer cell

evolution in the ovarian environment. The second argument is that this analysis may provide a list of highly specific biomarkers for each cancer. Indeed, this specific workflow allows for the comparison of the tissue types in their anatomical context. Each protein then is found in only one tissue and not in the other two. The confidence of this specificity is even higher because we compared gynecological tissues with each other. Indeed, it is difficult to attribute a gynecological disease biomarker to a specific organ.

We first determined the gene ontology of each protein specifically identified in serous or ovarian tissues and evaluated their molecular function. Figure 7A, B, C, and D shows the molecular functions and cellular processes of serous ovarian cancer and the molecular functions and the cellular processes of tubal cancer. We found that the molecular functions were not drastically different between the two tissues. The relative distributions of the functions were similar between the two cancers. This suggests that, although different proteins are implicated in fallopian tube tumorigenesis, the same biological mechanisms contribute to both neoplasms.

For example, molecular binding was highly represented in the two tissues. However, other molecular functions were listed for ovarian cancer including transmembrane transport and the peptidase function. Actin modeling, proliferation, and intercellular adhesion are the primary functions found in serous cancer. Here again, the most represented function was molecular binding.

However, by close inspection of the nature of the proteins specifically identified in serous ovarian cancer (Supporting Information Table 1), we observed that the proteins bearing binding functions were drastically different from the proteins found in common between ovarian and tubal cancer. Indeed, we found that the adhesion proteins overexpressed in ovarian tissue were proteins corresponding to epithelial differentiation. For example, cell–cell adhesion proteins, cell–cell adherent junction proteins, homophilic, and homotypic cell adhesion proteins were highly represented functions in this histological context. Some proteins implicated in cellular adhesion with the extracellular matrix were also found. The second striking observation was the high content of proteins implicated in cellular proliferation. Finally, many proteins associated with actin modeling appeared as an important overrepresented function among those proteins. These observations provide insights into the specific mechanisms we found in ovarian cancers. In fact, serous ovarian carcinogenesis appears to be controlled by highly specific mechanisms. These mechanisms may consist of the acquisition of epithelial characteristics combined with a great modeling of the cell shape and a greater proliferation potential. Other represented proteins are implicated in metabolism, HSP binding, lipid transport, and catabolism, and MAPK network activation. All of these events are in agreement with previous findings in ovarian cancer research [48].

We also used the Reactome NCI plugin to determine whether the proteins were previously characterized in ovarian neoplasms. The network of these proteins is presented in Fig. 7E (Supporting Information Table 4). Among these, we found the GTPases KRas [50] and NRas [51], mitogen-activated protein kinase 1 [52, 53], and receptor tyrosine-protein kinase erbB-2 [54, 55], which are involved in the epidermal growth factor receptor signaling pathway that greatly promotes ovarian cancer [56–58], resulting in cancer progression. Focal adhesion kinase 1 [59] is involved is the VEGF (vascular endothelial growth factor) receptor pathway, which promotes angiogenesis and the integrin pathway and induces the mitogen-activated protein kinase pathway [53], resulting in cancer progression. Fibronectin [60] is the extracellular component that activates the integrin pathway. The integrin pathway also induces actin polymerization for cellular remodeling [61]. In addition, metastasis-associated protein is involved in activating the p53 pathway [62].

Supporting Information Table 1 lists the proteins specifically identified in serous ovarian cancer, from the highest to lowest score. In this table, we determined that the most prevalent proteins corresponded to proteins associated with cellular shape changes [63], including cytoskeletal proteins, namely actin, beta actin like protein and microtubule-associated proteins. Proteins associated with nuclear modeling constituted another group of well-represented proteins, including histone H2B, histone H3, and heterochromatin protein 1-binding protein. The epigenetic modification of histones results in the repression of some genes and tumorigenesis events [64]. Among the highest scoring proteins, we also found those implicated in metabolism such as transketolase [65], which is implicated in the pentose-phosphate pathway that is often used in metastatic processes [48]. We also found proteins involved in glycolysis, which is another preferred metabolic pathway [66], including 6-phosphofructokinase and enolase. As previously mentioned, proteins involved in cell–cell interactions are represented, including zyxin [67] and desmoglein. Finally, we found that the majority of proteins implicated in RNA and protein synthesis were among the highest scoring. Among these proteins, we found heterogeneous nuclear ribonucleoproteins, ribosome-binding protein, eukaryotic translation initiation factor, protein disulfide-isomerase, 60 kDa SS-A/Ro ribonucleoprotein, and regulation of nuclear pre-mRNA domain-containing protein. All of these proteins had high scores in this analysis and may be considered for further analyses and validation by other methods using a large patients cohort. In this study, we determined the most important proteins specifically expressed in serous ovarian cancer.

We then investigated the specific tubal cancer biomarkers. The aim of this part of the study was to evaluate the relevance of the ovarian biomarkers for serous ovarian cancers. Indeed, if the ovarian cancer origin theory is valid, then tubal precursor markers may be appropriate for screening large cohorts of patients for the diagnosis of highly prevalent serous ovarian cancer. To do so, we used the Reactome NCI plugin to determine whether biomarkers initially discovered in the ovarian cancer context were expressed in fallopian tube tissues (Fig. 7F, Supporting Information Table 4). We observed

Clinical Relevance

With about 22 000 cases estimated in 2012 in the United States and 15 500 deaths, ovarian cancer is the fifth deadliest cancer among American women. Although some progress have been made by prolonging remission by the combination of aggressive surgery and chemotherapy, outcome for patients with ovarian cancer remains poor, with 5-year survival being about 30%. Possible reasons for the slow progress in the efficiency of treatment are the lack of early screening methods and the fact until recently that ovarian cancers have been considered as a unique entity. In fact, ovarian cancer is a general term for a series of molecular and aetiologically distinct diseases that share only an anatomical location. A better understanding of the molecular mechanisms underlying ovarian will permit several improvement of management of ovarian cancer. First, knowledge of the origin of the different ovarian cancer permits well-fitted prophylactic measures (e.g. salpingectomy for high-grade serous ovarian cancer, ablation of endometriotic lesions for clear cell ovarian carcinoma). Second, the description of molecular specificity of the proteins of each subtype will permit definition of early biomarkers, useful for early diagnosis. Third, molecular insights will identify therapeutic targets. Fourth, clinical trials should no longer aggregate the various ovarian types. Clinical reporting and scientific publications should use standardized terms for these entities. Fifth, improved experimental models must reflect the various originating cells and underlying genomic events driving each subtype.

that highly scoring proteins that were previously assigned to ovarian neoplasm were found in the fallopian tube tissue. This finding is the first clue that some biomarkers normally found in an ovarian cancer context may actually be tubal cancer biomarkers. Among these proteins, we found Fibronectin 1, which is implicated in the integrin pathway for actin remodeling [60]; cell division control protein 42, which is involved in cell migration [68]; the glycolysis enzyme gamma-enolase; high-mobility group protein 1 [69], which is involved in the facilitation of transcription, replication, recombination, and DNA repair. We also found some cell–cell junction proteins such as junction plakoglobin and alpha catenin a1 because tubal cancer is also an epithelial cancer; and serine/threonine-protein kinase PAK 1 [70] and integrin-linked protein kinase, which are involved in cytoskeleton remodeling [71].

This network is striking evidence that biomarkers initially found in the ovarian cancer context are also fallopian tube cancer biomarkers. This finding is reinforced by the fact that the Reactome NCI Plugin did not allow us to find tubal cancer biomarkers in the tubal cancer environment. Ovarian and tubal cancers evidently share biological functions in their development. However, the anatomical context provides a more accurate insight of the biomarkers for each gynecological disease.

Finally, we closely investigated the biological relevance of the highest scoring biomarkers in the fallopian tube environment to highlight the gynecological markers that the Reactome NCI Plugin may have missed.

Among all of the high scoring proteins found in the tubal tumoral environment, the most striking is periostin. This protein has been reported to be present in the environment of many cancer cells types. Periostin is a component of the extracellular matrix, and in cancer, it acts as a ligand for alpha-V/beta-3 and alpha-V/beta-5 integrins to support the adhesion and migration of epithelial cells [72]. The binding of this ligand also promotes the recruitment of the epidermal growth factor receptor and the activation of the Akt/PKB- and FAK-mediated signaling pathways [71]. Periostin-activated signaling pathways also promote cellular survival, angiogenesis, and resistance to hypoxia-induced cell death. In ovarian cancer, periostin promotes ovarian cancer angiogenesis and metastasis [72, 73]. In this particular case, we found periostin specifically expressed in the fallopian tube cancer environment and not in that of ovarian cancer. This is a highly important point for the understanding of the relevance of the adapted workflow. This specific approach, relying on tissue proteomics in an anatomical context, allowed us to determine that periostin was a tubal cancer protein that was not present in ovarian cancer. This also allows us to identify another response element to the question of ovarian cancer cellular origin. Here, we can speculate that periostin, which is highly expressed in tubal cancer, may induce the metastasis of fallopian tube cancer cells and promote their metastasis to a host tissue, which includes the ovary.

Osteopontin is another biomarker of the same type that promotes cell migration via integrin binding, and it has been previously found in epithelial ovarian cancers and was selected together with five other biomarkers for the multiplexed screening of epithelial ovarian cancers [74].

In this manner, ovarian serous cancers may develop after early metastasis events in the fallopian tube context from tubal cancer cells settling in the ovary. This theory is in agreement with the relative anatomical position of the fallopian tubes and the ovaries in the gynecological tracts. The fallopian tubes and the ovaries are physiologically closely related. For example, during reproduction events after ovulation, the female gamete migrates from the ovary to the endometrium through the fallopian tube. From this point of view, it is not

surprising that the preferred hosting site for a migrating tubal cancer cell would be the ovary.

It is now possible to link the events that we observed that are shared by the fallopian tubes and ovaries and specific ovarian cancer events. We found that the events shared between ovarian and fallopian tube cancers consisted of the downregulation of many proteins. Assuming that a serous ovarian cancer could be derived from a fallopian tube cancerous cell, it appears that in both cases, this cell may need to act as a molecular phantom in its anatomical context, which results from the suppression of immune proteins in the cancerous context. The adhesion of the cell to the extracellular matrix must then be suppressed for detachment for its tumoral context. This detachment would be promoted by extracellular matrix elements. In the ovarian environment, cell proliferation greatly increases. In addition, the cell may undergo many changes to acquire epithelial characteristics. This event is transduced by an important remodeling of the actin network of the cell and the expression of proteins mostly involved in cell–cell interactions. All of the proteins specifically found in the ovarian cancer context may represent pathological biomarkers. Indeed, membrane proteins that are in close contact with the extracellular milieu, which could easily be found in circulating fluids, must have a particular role in the transformation process.

We also demonstrated that some ovarian cancer biomarkers are actually fallopian tube cancer biomarkers. This discovery highlights the relevance of the anatomical context in the biomarkers research field. At the same time, this discovery suggests new methods for investigating the clinical screening of ovarian cancer.

4 Concluding remarks

Many questions remain regarding the origin of EOC and its mechanisms of progression. The emergence of proteomic technologies that identify potential biomarkers in body fluids and tissues allows biologists and clinicians to access pathological analysis on the molecular scale.

Here, we proposed a two-step strategy for the study of specific proteins in their histological context. The first step is a quick examination of the molecular profiles found in tissues that are of a different nature. The PCA calculation is based on a global comparison of multidimensional data. We applied these analyses to spectra groups using the relative intensities of the detected peaks in tissue sections. This experiment is a quick way to provide the complete molecular content trends of the histological regions of interest on a single or a few biopsied sections. PCA was used for the comparison of tissues in the same patient to avoid interpatient tissue variability. We speculated that the analysis of a small number of tissues may gain confidence when the patient is considered as the control in the experiment. The 2D representations provided by PCA allowed us to classify these in a way that our findings support the Müllerian origin of endometrioid and serous cancer hypothesis.

The second step consisted of a deeper investigation of the molecular actors in the tissues of interest. To do so, we performed a shotgun proteomics analysis of the tryptic digests analyzed on tissues with the MALDI source. The subsequent analyses using Blast2GO and Cytoscape softwares gave us a global view of the potential biological events that may occur during serous cancer development. If we assume that serous epithelial ovarian cancers originate from a fallopian tube cancerous precursor, then cell detachment mechanisms from the tumor site may be involved as an immunosuppression mechanism for a cell that is considered a foreign element in the physiological context. In the ovarian environment, additional specific events may occur. The newly settled and undifferentiated cell may differentiate into an epithelial cell to form an epithelial cancer in the ovarian host site.

This type of experiment can provide important insights into the histological specificity of the proteins of each pathology. We introduce a new concept that consists of providing new evidence for a clinical problem while assessing the molecular specificity of the pathological proteins. Based on the relative scores of the proteins found in different tissues, we were able to assess the relative specificity of the proteins in each tissue. We then provided the first proteomic insight into the degree of similarity of the serous ovarian cancer tissues with its possibly related Müllerian tissue. This comparison allowed us to elucidate the possible molecular mechanisms found in the appearance of ovarian cancer and its development.

Determining the specific serous epithelial ovarian cancer markers is only possible using this specific tissue profiling workflow. This may be considered for specific tissue biomarkers studies. The proteins upregulated in each tissue may be selected for their specificity against two or more tissues from the same patient. Indeed, the clinical value of a biomarker that is useable for a diagnostic test is its specificity for one cancer type as opposed to another. Here, we propose a list of specific serous ovarian cancer proteins that are found in their anatomical context and guaranteed to be absent in normal ovarian tissue and another type of gynecological cancer from the same patient, i.e. the fallopian tube. Thus, these proteins are specific to the cancerous pathological status and are specific for the ovary as opposed to other gynecologic neoplasms.

The scope of this type of analysis is to evaluate the most appropriate biomarkers for serous ovarian cancer. If the fallopian tube is the cause of ovarian cancer, a large campaign identifying the fallopian tube cancer biomarkers may be performed. This may provide an insight into the early development of this specific neoplasm and identify the precise time when radical fimbriectomy may be performed for at-risk or even nonsuspecting patients.

To definitively validate the hypotheses and biomarkers found, it will be necessary to repeat this experiment in a large cohort of tissues and interpret the results using statistical analyses. However, using the same patient for a comparison analysis is an excellent internal control for the experiment.

At this time, we speculate that the observations made after this study may be the cornerstone of the Müllerian origin of serous ovarian cancer theory.

In conclusion, this workflow is an example of the potential of the mass spectrometric profiling method for biomarker research and for specific clinical application. We have been able to prove the feasibility of this method while providing the first proteomic evidence of the potential tubal origin of serous ovarian cancer. We also introduced a new research method for the investigation of gynecological cancer biomarkers. On-tissue proteomics allowed us to determine that ovarian cancer biomarkers may actually derive from fallopian tube cancer precursors; it may then be relevant to compare whether biomarkers found in fallopian tube cancers have good predictive values for ovarian cancer screening in large patient cohorts. This type of investigation may be highly relevant for the early detection of ovarian cancers.

This research was supported by a collaboration between The Fundamental and Applied Biology Mass Spectrometry laboratory (M.S.) and Thermofisher (Bremen, K.S.) and grants from the Centre National de la Recherche Scientifique (CNRS), Ministère de L'Education Nationale, de L'Enseignement Supérieur et de la Recherche, Agence Nationale de la Recherche (ANR PCV to I.F.), Canadian Institutes of Health Research (CIHR to M.S. and R.D.), Ministère du Développement Économique de l'Innovation et de l'Exportation (MDEIE to R.D.), Fonds de Recherche du Québec – Santé (FRQS to R.D.), CHRU of Lille (to C.B.), CNRS for HG and Région Nord-Pas de Calais and Université de Sherbrooke (to R.L.). R.D. is a member of the Centre de Recherche Clinique Etienne-Le Bel (Sherbrooke, QC, Canada).

The authors have declared no conflict of interest.

5 References

[1] Dubeau, L., The cell of origin of ovarian epithelial tumours. *Lancet Oncol.* 2008, *9*, 1191–1197.

[2] Shih Ie, M., Kurman, R. J., Ovarian tumorigenesis: a proposed model based on morphological and molecular genetic analysis. *Am. J. Pathol.* 2004, *164*, 1511–1518.

[3] Bell, D. A., Scully, R. E., Early de novo ovarian carcinoma. A study of fourteen cases. *Cancer* 1994, *73*, 1859–1864.

[4] Leblanc, E., Narducci, F., Farre, I., Peyrat, J. P. et al., Radical fimbriectomy: a reasonable temporary risk-reducing surgery for selected women with a germ line mutation of BRCA 1 or 2 genes? Rationale and preliminary development. *Gynecol. Oncol.* 2011, *121*, 472–476.

[5] Callahan, M. J., Crum, C. P., Medeiros, F., Kindelberger, D. W. et al., Primary fallopian tube malignancies in BRCA-positive women undergoing surgery for ovarian cancer risk reduction. *J. Clin. Oncol.* 2007, *25*, 3985–3990.

[6] Carcangiu, M. L., Radice, P., Manoukian, S., Spatti, G. et al., Atypical epithelial proliferation in fallopian tubes in prophylactic salpingo-oophorectomy specimens from BRCA1 and BRCA2 germline mutation carriers. *Int. J. Gynecol. Pathol.* 2004, *23*, 35–40.

[7] Colgan, T. J., Murphy, J., Cole, D. E., Narod, S., Rosen, B., Occult carcinoma in prophylactic oophorectomy specimens: prevalence and association with BRCA germline mutation status. *Am. J. Surg. Pathol.* 2001, *25*, 1283–1289.

[8] Finch, A., Shaw, P., Rosen, B., Murphy, J. et al., Clinical and pathologic findings of prophylactic salpingo-oophorectomies in 159 BRCA1 and BRCA2 carriers. *Gynecol. Oncol.* 2006, *100*, 58–64.

[9] Kindelberger, D. W., Lee, Y., Miron, A., Hirsch, M. S., Intraepithelial carcinoma of the fimbria and pelvic serous carcinoma: evidence for a causal relationship. *Am. J. Surg. Pathol.* 2007, *31*, 161–169.

[10] Piek, J. M., van Diest, P. J., Zweemer, R. P., Kenemans, P, Verheijen, R. H., Tubal ligation and risk of ovarian cancer. *Lancet* 2001, *358*, 844.

[11] Piek, J. M., Verheijen, R. H., Kenemans, P., Massuger, L. F. et al., BRCA1/2-related ovarian cancers are of tubal origin: a hypothesis. *Gynecol. Oncol.* 2003, *90*, 491.

[12] Shaw, P. A., Rouzbahman, M., Pizer, E. S., Pintilie, M., Begley, H., Candidate serous cancer precursors in fallopian tube epithelium of BRCA1/2 mutation carriers. *Mod. Pathol.* 2009, *22*, 1133–1138.

[13] Staebler, A., Preneoplasias of ovarian carcinoma: biological and clinical aspects of different pathways of tumorigenesis. *Pathologe* 2011, *32* (Suppl 2), 265–270.

[14] Leonhardt, K., Einenkel, J., Sohr, S., Engeland, K., Horn, L. C., p53 signature and serous tubal in-situ carcinoma in cases of primary tubal and peritoneal carcinomas and serous borderline tumors of the ovary. *Int. J. Gynecol. Pathol.* 2011, *30*, 417–424.

[15] Chen, E. Y., Mehra, K., Mehrad, M., Ning, G., Secretory cell outgrowth, PAX2 and serous carcinogenesis in the fallopian tube. *J. Pathol.* 2011, *222*, 110–116.

[16] Carlson, J. W., Jarboe, E. A., Kindelberger, D., Nucci, M. R. et al., Serous tubal intraepithelial carcinoma: diagnostic reproducibility and its implications. *Int. J. Gynecol. Pathol.* 2010, *29*, 310–314.

[17] Wei, C. F., Hwang, S. H., Ho, C. M., Shih, B. Y., Chien, T. Y., Malignant mixed mullerian tumors of the ovary. *Zhonghua Yi Xue Za Zhi (Taipei)* 2000, *63*, 344–348.

[18] Roh, M. H., Kindelberger, D., Crum, C. P., Serous tubal intraepithelial carcinoma and the dominant ovarian mass: clues to serous tumor origin? *Am. J. Surg. Pathol.* 2009, *33*, 376–383.

[19] Jarboe, E., Folkins, A., Nucci, M. R., Kindelberger, D. et al., Serous carcinogenesis in the fallopian tube: a descriptive classification. *Int. J. Gynecol. Pathol.* 2008, *27*, 1–9.

[20] Stoeckli, M., Chaurand, P., Hallahan, D. E., Caprioli, R. M., Imaging mass spectrometry: a new technology for the analysis of protein expression in mammalian tissues. *Nat. Med.* 2001, *7*, 493–496.

[21] Callesen, A. K., Vach, W., Jorgensen, P. E., Cold, S. et al., Reproducibility of mass spectrometry based protein profiles

for diagnosis of breast cancer across clinical studies: a systematic review. *J. Proteome Res.* 2008, *7*, 1395–1402.

[22] Franck, J., Arafah, K., Elayed, M., Bonnel, D. et al., MALDI imaging mass spectrometry: state of the art technology in clinical proteomics. *Mol. Cell. Proteomics* 2009, *8*, 2023–2033.

[23] Schwartz, S. A., Weil, R. J., Thompson, R. C., Shyr, Y. et al., Proteomic-based prognosis of brain tumor patients using direct-tissue matrix-assisted laser desorption ionization mass spectrometry. *Cancer Res.* 2005, *65*, 7674–7681.

[24] Fournier, I., Day, R., Salzet, M., Direct analysis of neuropeptides by in situ MALDI-TOF mass spectrometry in the rat brain. *Neuro. Endocrinol. Lett.* 2003, *24*, 9–14.

[25] Fournier, I., Wisztorski, M., Salzet, M., Tissue imaging using MALDI-MS: a new frontier of histopathology proteomics. *Expert Rev. Proteomics* 2008, *5*, 413–424.

[26] El Ayed, M., Bonnel, D., Longuespee, R., Castellier, C. et al., MALDI imaging mass spectrometry in ovarian cancer for tracking, identifying, and validating biomarkers. *Med. Sci. Monit.* 2010, *16*, BR233–BR245.

[27] Franck, J., Longuespee, R., Wisztorski, M., Van Remoortere, A. et al., MALDI mass spectrometry imaging of proteins exceeding 30,000 daltons. *Med. Sci. Monit.* 2010, *16*, BR293–BR299.

[28] Lemaire, R., Lucot, J. P., Collinet, P., Vinatier, D. et al., New developments in direct analyses by MALDI mass spectrometry for study ovarian cancer. *Mol. Cell Proteomics* 2005, *4*, S305–S308.

[29] Lemaire, R., Menguellet, S. A., Stauber, J., Marchaudon, V. et al., Specific MALDI imaging and profiling for biomarker hunting and validation: fragment of the 11S proteasome activator complex, Reg alpha fragment, is a new potential ovary cancer biomarker. *J. Proteome Res.* 2007, *6*, 4127–4134.

[30] Longuespee, R., Boyon, C., Castellier, C. et al., The C-terminal fragment of the immunoproteasome PA28S (Reg alpha) as an early diagnosis and tumor-relapse biomarker: evidence from mass spectrometry profiling. *Histochem Cell Biol.* 2012, *138*, 141–154.

[31] Stauber, J., Lemaire, R., Wisztorski, M., Ait-Menguellet, S. et al., New developments in MALDI imaging mass spectrometry for pathological proteomic studies; introduction to a novel concept, the specific MALDI imaging. *Mol. Cell Proteomics* 2006, *5*, S247–S249.

[32] Bonnel, D., Legouffe, R., Willand, N., Baulard, A. et al., MALDI imaging techniques dedicated to drug-distribution studies. *Bioanalysis* 2011, *3*, 1399–1406.

[33] Bonnel, D., Longuespee, R., Franck, J., Roudbaraki, M. et al., Multivariate analyses for biomarkers hunting and validation through on-tissue bottom-up or in-source decay in MALDI-MSI: application to prostate cancer. *Anal. Bioanal. Chem.* 2011, *401*, 149–165.

[34] Gustafsson, J. O., Oehler, M. K., McColl, S. R., Hoffmann, P., Citric acid antigen retrieval (CAAR) for tryptic peptide imaging directly on archived formalin-fixed paraffin-embedded tissue. *J. Proteome Res.* 2010, *9*, 4315–4328.

[35] Franck, J., Arafah, K., Barnes, A., Wisztorski, M. et al., Improving tissue preparation for matrix-assisted laser desorption ionization mass spectrometry imaging. Part 1: using microspotting. *Anal. Chem.* 2009, *81*, 8193–8202.

[36] Lemaire, R., Desmons, A., Tabet, J. C., Day, R. et al., Direct analysis and MALDI imaging of formalin-fixed, paraffin-embedded tissue sections. *J. Proteome Res.* 2007, *6*, 1295–1305.

[37] Deininger, S. O., Ebert, M. P., Futterer, A., Gerhard, M., Rocken, C., MALDI imaging combined with hierarchical clustering as a new tool for the interpretation of complex human cancers. *J. Proteome Res.* 2008, *7*, 5230–5236.

[38] Dauly, C., Fréret, M., Drouot, L., Ho, J. T. C. et al., High-resolution targeted quantitation: biomarker discovery in a mouse transgenic model of myopathy, application note 555, thermo. *Fisher Scientific* 2011.

[39] Colinge, J., Chiappe, D., Lagache, S., Moniatte, M., Bougueleret, L., Differential proteomics via probabilistic peptide identification scores. *Anal. Chem.* 2005, *77*, 596–606.

[40] Nanduri, B., Lawrence, M. L., Vanguri, S., Pechan, T., Burgess, S. C., Proteomic analysis using an unfinished bacterial genome: the effects of subminimum inhibitory concentrations of antibiotics on *Mannheimia haemolytica* virulence factor expression. *Proteomics* 2005, *5*, 4852–4863.

[41] Searle, B. C., Scaffold: a bioinformatic tool for validating MS/MS-based proteomic studies. *Proteomics* 2010, *10*, 1265–1269.

[42] Conesa, A., Gotz, S., Garcia-Gomez, J. M., Terol, J. et al., Blast2GO: a universal tool for annotation, visualization and analysis in functional genomics research. *Bioinformatics* 2005, *21*, 3674–3676.

[43] Szklarczyk, D., Franceschini, A., Kuhn, M., Simonovic, M. et al., The STRING database in 2011: functional interaction networks of proteins, globally integrated and scored. *Nucleic Acids Res.* 2011 *39*, D561–D568.

[44] Smoot, M. E., Ono, K., Ruscheinski, J., Wang, P. L., Ideker, T., Cytoscape 2.8: new features for data integration and network visualization. *Bioinformatics* 2011, *27*, 431–432.

[45] Djidja, M. C., Carolan, V., Loadman, P. M., Clench, M. R., Method development for protein profiling in biological tissues by matrix-assisted laser desorption/ionisation mass spectrometry imaging. *Rapid Commun. Mass Spectrom.* 2008, *22*, 1615–1618.

[46] Trim, P. J., Henson, C. M., Avery, J. L., McEwen, A. et al., Matrix-assisted laser desorption/ionization-ion mobility separation-mass spectrometry imaging of vinblastine in whole body tissue sections. *Anal. Chem.* 2008, *80*, 8628–8634.

[47] Prat, J., New insights into ovarian cancer pathology. *Ann. Oncol.* 2012, *23*(Suppl 10), x111–x117.

[48] Longuespee, R., Boyon, C., Desmons, A. et al., Ovarian cancer molecular pathology. *Cancer Metastasis Rev.* 2012, *31*, 713–732.

[49] Longuespee, R., Boyon, C., Castellier, C., Jacquet, A. et al., The *C*-terminal fragment of the immunoproteasome PA28S (Reg alpha) as an early diagnosis and tumor-relapse biomarker: evidence from mass spectrometry profiling. *Histochem. Cell Biol.* 2012, *138*, 141–154.

[50] Ratner, E. S., Keane, F. K., Lindner, R. A., Tassi, R. A. et al., A KRAS variant is a biomarker of poor outcome, platinum chemotherapy resistance and a potential target for therapy in ovarian cancer. *Oncogene*, 2012, *31*, 4559–4566.

[51] Meunier, L., Puiffe, M. L., Le Page, C., Filali-Mouhim, A. et al., Effect of ovarian cancer ascites on cell migration and gene expression in an epithelial ovarian cancer in vitro model. *Transl. Oncol.* 2010, *3*, 230–238.

[52] Nonaka, M., Itamochi, H., Kawaguchi, W., Kudoh, A. et al., Activation of the mitogen-activated protein kinase kinase/extracellular signal-regulated kinase pathway overcomes cisplatin resistance in ovarian carcinoma cells. *Int. J. Gynecol. Cancer* 2012, *22*, 922–929.

[53] Roberts, P. J., Der, C. J., Targeting the Raf-MEK-ERK mitogen-activated protein kinase cascade for the treatment of cancer. *Oncogene* 2007, *26*, 3291–3310.

[54] Wilken, J. A., Badri, T., Cross, S., Raji, R. et al., EGFR/HER-targeted therapeutics in ovarian cancer. *Future Med. Chem.* 2012, *4*, 447–469.

[55] Felip, E., Del Campo, J. M., Rubio, D., Vidal, M. T. et al., Overexpression of c-erbB-2 in epithelial ovarian cancer. Prognostic value and relationship with response to chemotherapy. *Cancer* 1995, *75*, 2147–2152.

[56] Zhou, C., Qiu, L., Sun, Y., Healey, S. et al., Inhibition of EGFR/PI3K/AKT cell survival pathway promotes TSA's effect on cell death and migration in human ovarian cancer cells. *Int. J. Oncol.* 2006, *29*, 269–278.

[57] Kandala, P. K., Wright, S. E., Srivastava S. K. Blocking epidermal growth factor receptor activation by 3,3′-diindolylmethane suppresses ovarian tumor growth in vitro and in vivo. *J. Pharmacol. Exp. Ther.* 2012, *341*, 24–32.

[58] Sheng, Q., Liu, J., The therapeutic potential of targeting the EGFR family in epithelial ovarian cancer. *Br. J. Cancer* 2011, *104*, 1241–1245.

[59] Judson, P. L., He, X., Cance, W. G., Van Le, L., Overexpression of focal adhesion kinase, a protein tyrosine kinase, in ovarian carcinoma. *Cancer* 1999, *86*, 1551–1556.

[60] Xing, H., Weng, D., Chen, G., Tao, W. et al., Activation of fibronectin/PI-3K/Akt2 leads to chemoresistance to docetaxel by regulating survivin protein expression in ovarian and breast cancer cells. *Cancer Lett.* 2008, *261*, 108–119.

[61] Vicente-Manzanares, M., Choi, C. K., Horwitz, A. R., Integrins in cell migration—the actin connection. *J. Cell Sci.* 2009, *122*, 199–206.

[62] Li, D. Q., Divijendra Natha Reddy, S., Pakala, S. B., Wu, X. et al., MTA1 coregulator regulates p53 stability and function. *J. Biol. Chem.* 2009, *284*, 34545–34552.

[63] Creekmore, A. L., Silkworth, W. T., Cimini, D., Jensen, R. V. et al., Changes in gene expression and cellular architecture in an ovarian cancer progression model. *PLoS One* 2011, *6*, e17676.

[64] Seeber, L. M., van Diest, P. J., Epigenetics in ovarian cancer. *Methods Mol. Biol.* 2012, *863*, 253–269.

[65] Krockenberger, M., Honig, A., Rieger, L., Coy, J. F. et al., Transketolase-like 1 expression correlates with subtypes of ovarian cancer and the presence of distant metastases. *Int. J. Gynecol. Cancer* 2007, *17*, 101–106.

[66] Karantanis, D., Allen-Auerbach, M., Czernin, J., Relationship among glycolytic phenotype, grade, and histological subtype in ovarian carcinoma. *Clin. Nucl. Med.* 2012, *37*, 49–53.

[67] Grunewald, T. G., Kammerer, U., Winkler, C., Schindler, D. et al., Overexpression of LASP-1 mediates migration and proliferation of human ovarian cancer cells and influences zyxin localisation. *Br. J. Cancer* 2007, *96*, 296–305.

[68] Mythreye, K., Blobe, G. C., The type III TGF-beta receptor regulates epithelial and cancer cell migration through beta-arrestin2-mediated activation of Cdc42. *Proc. Natl. Acad. Sci. USA* 2009, *106*, 8221–8216.

[69] Chen, J., Xi, B., Zhao, Y., Yu, Y. et al., High-mobility group protein B1 (HMGB1) is a novel biomarker for human ovarian cancer. *Gynecol. Oncol.* 2012, *126*, 109–117.

[70] Siu, M. K., Wong, E. S., Chan, H. Y., Kong, D. S. et al., Differential expression and phosphorylation of Pak1 and Pak2 in ovarian cancer: effects on prognosis and cell invasion. *Int. J. Cancer* 2010, *127*, 21–31.

[71] Lin, S. W., Ke, F. C., Hsiao, P. W., Lee, P. P. et al., Critical involvement of ILK in TGFbeta1-stimulated invasion/migration of human ovarian cancer cells is associated with urokinase plasminogen activator system. *Exp. Cell Res.* 2007, *313*, 602–613.

[72] Gillan, L., Matei, D., Fishman, D. A., Gerbin, C. S. et al., Periostin secreted by epithelial ovarian carcinoma is a ligand for alpha(V)beta(3) and alpha(V)beta(5) integrins and promotes cell motility. *Cancer Res.* 2002, *62*, 5358–5364.

[73] Zhu, M., Fejzo, M. S., Anderson, L., Dering, J. et al., Periostin promotes ovarian cancer angiogenesis and metastasis. *Gynecol. Oncol.* 2010, *119*, 337–344.

[74] Kim, K., Visintin, I., Alvero, A. B., Mor, G., Development and validation of a protein-based signature for the detection of ovarian cancer. *Clin. Lab. Med.* 2009, *29*, 47–55.

